

Published in final edited form as:

Chem Mater. ; 29(7): 2669–2671. doi:10.1021/acs.chemmater.6b04649.

Fluorinated polyurethane scaffolds for ^{19}F magnetic resonance imaging

Twan Lammers^{#1,2,†}, Marianne E. Mertens^{#1}, Philipp Schuster^{#3}, Khosrow Rahimi⁴, Yang Shi¹, Volkmar Schulz¹, Alexander J. C. Kuehne⁴, Stefan Jockenhoevel³, and Fabian Kiessling^{1,†}

¹Institute for Experimental Molecular Imaging, RWTH Aachen University Clinic, Pauwelsstrasse 30, 52074 Aachen, Germany ²Department of Targeted Therapeutics, University of Twente, PO Box 217, 7500 AE Enschede, The Netherlands ³Department of Biohybrid and Medical Textiles, AME-Helmholtz Institute for Biomedical Engineering and ITA-Institute for Textile Technology, RWTH Aachen University, Pauwelsstrasse 20, 52074 Aachen, Germany ⁴DWI-Leibniz Institute for Interactive Materials, Forckenbeckstrasse 50, 52074 Aachen, Germany

[#] These authors contributed equally to this work.

Abstract

Polymers are increasingly employed in implant materials. To reduce the incidence of complications, which in the case of vascular grafts include incorrect placement and restenosis, materials are needed which allow for image-guided implantation, as well as for accurate and efficient postoperative implant imaging. We here describe amorphous fluorinated polymers based on thermoplastic polyurethane (^{19}F -TPU), and show that are useful starting materials for developing tissue-engineered vascular grafts which can be detected using ^{19}F MRI.

Non-invasive imaging plays an increasingly important role in regenerative medicine. The direct visualization of implants using magnetic resonance imaging (MRI) can provide longitudinal feedback on the position, functionality, resorption and remodeling of the material. It also helps to identify collapsed or damaged regions in vascular grafts, and facilitates decision-making with respect to pharmacological or surgical interventions.

Besides the advantages of standard ^1H MRI, which include high spatial resolution, very good soft-tissue contrast and lack of ionizing radiation, ^{19}F MRI offers additional advantages.^{1,2} First and foremost, since there are hardly any endogenous fluorine atoms in the body (high levels are only found in teeth), the background MRI signal is very low, enabling 'hot spot' imaging and highly specific implant detection. The absence of background signals also allows for accurate and efficient quantification. A further advantage of ^{19}F MRI (over labeling with superparamagnetic iron oxide nanoparticles and standard ^1H MR imaging of implants^{3,4}) is the absence of susceptibility artifacts, which can disturb the analysis of adjacent tissues and of remodeling processes within the vascular graft.

[†] Corresponding authors (tlammers@ukaachen.de; fkiessling@ukaachen.de).

Fluorinated scaffold materials are consequently considered to be interesting starting materials for developing image-guided tissue-engineered vascular grafts.

Commonly used fluorinated polymers, such as polytetrafluoro-ethylene (PTFE; Teflon; GoreTex) and polyvinylidene fluoride (PVDF) cannot be employed for ^{19}F MRI, because their high crystallinity compromises the molecular mobility of the signal-producing fluorine atoms. As a consequence, even at ultra-short echo times, hardly any MRI signals are generated and the signals decay very fast, leading to poor sensitivity and prohibiting image acquisition (Figure 1). To enable ^{19}F MR imaging of scaffold materials, we generated a novel fluorinated polymer based on thermoplastic polyurethane (^{19}F -TPU) which possesses distinct properties rendering it suitable for fluorine-based MRI: (i) it possesses a large number of magnetically equivalent ^{19}F atoms, yielding strong resonance peaks; (ii) it has an amorphous structure, resulting in high mobility of the incorporated ^{19}F atoms; and (iii) it has favorable relaxation properties to achieve relatively long echo times.

The ^{19}F -TPU is synthesized from a perfluorinated aromatic diisocyanate and butanediol. After polymerization, the polyurethane is N-alkylated to obtain a non-crystalline material with partially fluorinated alkyl side chains (Figure 2A and Scheme S1). The average size of the final polymeric material was 7.4×10^3 Da (M_n ; $M_w = 1.5 \times 10^4$), and the polydispersity 2.0. It is known that PVDF exhibits high crystallinity (see DSC and XRD spectra in Figure S1 and S2). In order to model a spinning process, PVDF was heated to $T = 210$ °C, which is above T_m (~180 °C as determined by DSC in Figure S1), followed by subsequent cooling to room temperature. After this thermal treatment, PVDF retains its high crystallinity, which was verified using DSC and wide-angle X-ray scattering (WAXS) analysis (Figure 2D). Conversely, ^{19}F -TPU remained largely amorphous after the same thermal treatment (Figure 2C and S1).

Due to their amorphous nature, ^{19}F -TPU polymers have a much higher chain mobility than crystalline PVDF polymers. Therefore, the fluorine atoms in ^{19}F -TPU are less confined and can more efficiently tumble within the amorphous structure of the polymer. As a result, the fluorine atoms in ^{19}F -TPU generate two resonance peaks at -83.6 ppm and -123.5 ppm with favorable relaxation times ($T_1 = 225 \pm 6$ ms; $T_2 = 0.76 \pm 0.04$ ms; Figure 3A-C). The separation of both resonances enables undisturbed excitation and subsequent image readout of a single resonance, preventing the occurrence of artifacts. The generation of strong and specific ^{19}F MRI signals with slow signal decay permits background-free imaging of ^{19}F -TPU at clinically relevant settings, i.e. in a 3T patient scanner, at a relatively short acquisition time (<3 min), with a good signal-to-noise ratio (>10) and with a relatively high image resolution (<1 mm isotropic voxel size) (Figure 3D).

To provide proof-of-principle for the usefulness of ^{19}F -TPU for developing MRI-detectable scaffold materials, it was processed into monofilaments via melt spinning. Therefore, ^{19}F -TPU pellets were introduced into a twin-screw extruder and spun into monofilaments at a process temperature of 225-230°C. Subsequently, a vascular graft with a diamond braid and twelve monofilaments was produced. The braided structure had a braiding angle of 33° and its inner diameter was 6 mm. The resulting scaffold was imaged in a clinical 3T MRI scanner using a dual-tuned ($^{19}\text{F}/^1\text{H}$) volume coil and ultra-short echo time (UTE) sequences

with an echo/repetition time of 0.12/100 ms and a flip angle of 67°. Afterwards, the ^{19}F imaging data was 3D-rendered and overlaid with a ^1H image to demonstrate ‘hot spot’ MR imaging (Figure 4).

These findings indicate that ^{19}F -TPU can be utilized to develop MR imageable cardiovascular implants, enabling a detailed visualization of the architecture of vascular grafts and their unambiguous identification upon in vivo implantation. In recent years, several other fluorine-containing materials have been developed for ^{19}F MRI, but thus far only for functional and molecular imaging applications^{6–11}, for monitoring drug delivery¹², for cell tracking^{13,14} and for visualizing encapsulated cellular therapeutics^{15,16}. We here for the first time provide proof-of-principle for the generation of ^{19}F MRI-detectable polymeric scaffolds, which can be used as a starting material to develop imageable vascular grafts, and which may serve as a basis for theranostic tissue engineering.

Supporting information

Refer to Web version on PubMed Central for supplementary material.

Acknowledgements

The authors gratefully acknowledge Rainer Haas (DWI) for performing the GPC analysis. This work is financially supported by the NRW/EU-Ziel 2-Programm (EFRE) 2007-2013: “Entwicklung und Bildgebung patientenoptimierter Implantate”, by the Helmholtz-Society Portfolio Grant “Technologie und Medizin: Multimodale Bildgebung zur Aufklärung des In-vivo-Verhaltens von polymeren Biomaterialien”, by the European Research Council (ERC Starting Grant 309495: NeoNaNo), and by the ERS Boost Fund Program at RWTH Aachen University.

References

- (1). Ruiz-Cabello J, Barnett BP, Bottomley PA, Bulte JWM. Fluorine (^{19}F) MRS and MRI in biomedicine. *NMR Biomed.* 2011; 24:114–129. [PubMed: 20842758]
- (2). Tirota I, Dichiarante V, Pigliacelli C, Cavallo G, Terraneo G, Bombelli FB, Metrangolo P, Resnati G. (^{19}F) magnetic resonance imaging (MRI): from design of materials to clinical applications. *Chem Rev.* 2015; 115:1106–1129. [PubMed: 25329814]
- (3). Mertens ME, Hermann A, Bühren A, Olde-Damink L, Ehling J, Kiessling F, Lammers L. Iron oxide-labeled collagen scaffolds for non-invasive MR imaging in tissue engineering. *Adv Funct Mater.* 2014; 24:754–62. [PubMed: 24569840]
- (4). Reiss S, Krafft AJ, Zehender M, Heidt T, Pfannebecker T, Bode C, Bock M, von zur Muhlen C. Magnetic resonance imaging of bioresorbable vascular scaffolds: potential approach for noninvasive evaluation of coronary patency. *Circ Cardiovasc Interv.* 2015; 8:e002388. [PubMed: 25794509]
- (5). Mertens ME, Koch S, Schuster P, Wehner J, Wu Z, Gremse F, Schulz V, Rongen L, Wolf F, Frese J, Gesché VN, et al. USPIO-labeled textile materials for non-invasive MR imaging of tissue-engineered vascular grafts. *Biomaterials.* 2015; 39:155–163. [PubMed: 25465443]
- (6). Mizukami S, Takikawa R, Sugihara F, Hori Y, Tochio H, Wälchli M, Shirakawa M, Kikuchi K. Paramagnetic relaxation-based ^{19}F MRI probe to detect protease activity. *J Am Chem Soc.* 2008; 130:794–795. [PubMed: 18154336]
- (7). Mizukami S, Takikawa R, Sugihara F, Shirakawa M, Kikuchi K. Dual-function probe to detect protease activity for fluorescence measurement and ^{19}F MRI. *Angew Chem Int Ed.* 2009; 48:3641–3643.

- (8). Jiang ZX, Liu X, Jeong EK, Yu YB. Symmetry-guided design and fluororous synthesis of a stable and rapidly excreted imaging tracer for (19)F MRI. *Angew Chem Int Ed Engl.* 2009; 48:4755–4758. [PubMed: 19475598]
- (9). Thurecht KJ, Blakey I, Peng H, Squires O, Hsu S, Alexander C, Whittaker AK. Functional hyperbranched polymers: toward targeted in vivo 19F magnetic resonance imaging using designed macromolecules. *J Am Chem Soc.* 2010; 132:5336–5337. [PubMed: 20345132]
- (10). Tirotta I, Mastropietro A, Cordiglieri C, Gazzera L, Baggi F, Baselli G, Bruzzone MG, Zucca I, Cavallo G, Terraneo G, Baldelli Bombelli F, et al. A superfluorinated molecular probe for highly sensitive in vivo(19)F-MRI. *J Am Chem Soc.* 2014; 136:8524–8527. [PubMed: 24884816]
- (11). Temme S, Grapentin C, Quast C, Jacoby C, Grandoch M, Ding Z, Owenier C, Mayenfels F, Fischer JW, Schubert R, Schrader J, et al. Noninvasive imaging of early venous thrombosis by 19F magnetic resonance imaging with targeted perfluorocarbon nanoemulsions. *Circulation.* 2015; 131:1405–1414. [PubMed: 25700177]
- (12). Langereis S, Keupp J, van Velthoven JL, de Roos IH, Burdinski D, Pikkemaat JA, Gröll H. A temperature-sensitive liposomal 1H CEST and 19F contrast agent for MR image-guided drug delivery. *J Am Chem Soc.* 2009; 131:1380–1381. [PubMed: 19173663]
- (13). Srinivas M, Heerschap A, Ahrens ET, Figdor CG, de Vries IJ. (19)F MRI for quantitative in vivo cell tracking. *Trends Biotechnol.* 2010; 28:363–370. [PubMed: 20427096]
- (14). Srinivas M, Boehm-Sturm P, Figdor CG, de Vries IJ, Hoehn M. Labeling cells for in vivo tracking using (19)F MRI. *Biomaterials.* 2012; 33:8830–8840. [PubMed: 22959182]
- (15). Barnett BP, Ruiz-Cabello J, Hota P, Liddell R, Walczak P, Howland V, Chacko VP, Kraitchman DL, Arepally A, Bulte JW. Fluorocapsules for improved function, immunoprotection, and visualization of cellular therapeutics with MR, US, and CT imaging. *Radiology.* 2011; 258:182–191. [PubMed: 20971778]
- (16). Barnett BP, Arepally A, Stuber M, Arifin DR, Kraitchman DL, Bulte JW. Synthesis of MR-, X-ray- and US-visible alginate microcapsules for immunoisolation and noninvasive imaging of cellular therapeutics. *Nat Protoc.* 2011; 6:1142–1151. [PubMed: 21799484]

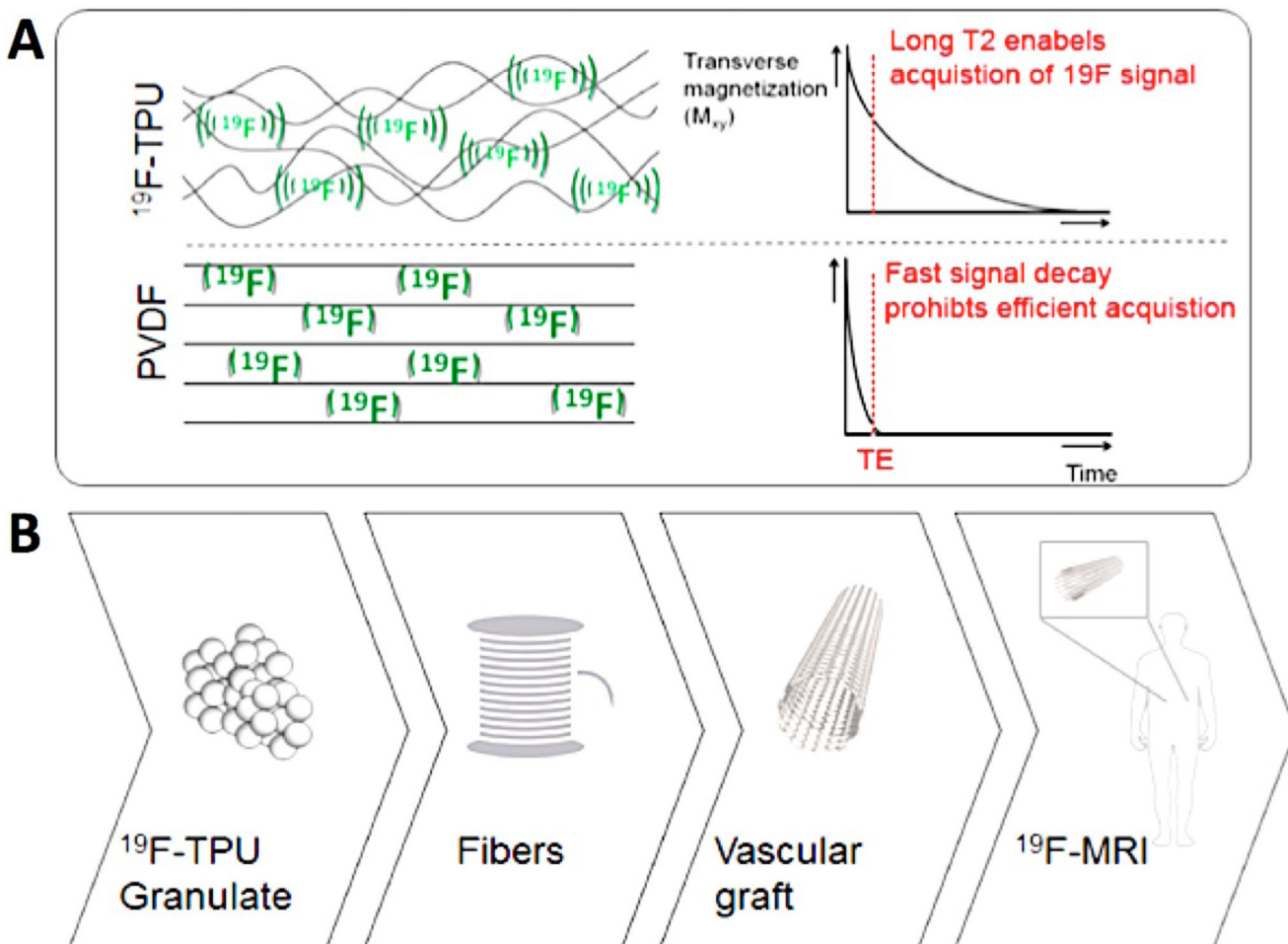


Figure 1.

Fluorinated polymers for ^{19}F MRI. A: The amorphous structure of ^{19}F -TPU results in high mobility of fluorine atoms and in long T_2 relaxation times, enabling efficient MR image acquisition. Conversely, the high crystallinity of PVDF leads to short echo times, fast signal decay and short T_2 . B: ^{19}F -TPU was used to prepare polymeric fibers, which were braided into vascular scaffold materials enabling ^{19}F MRI.

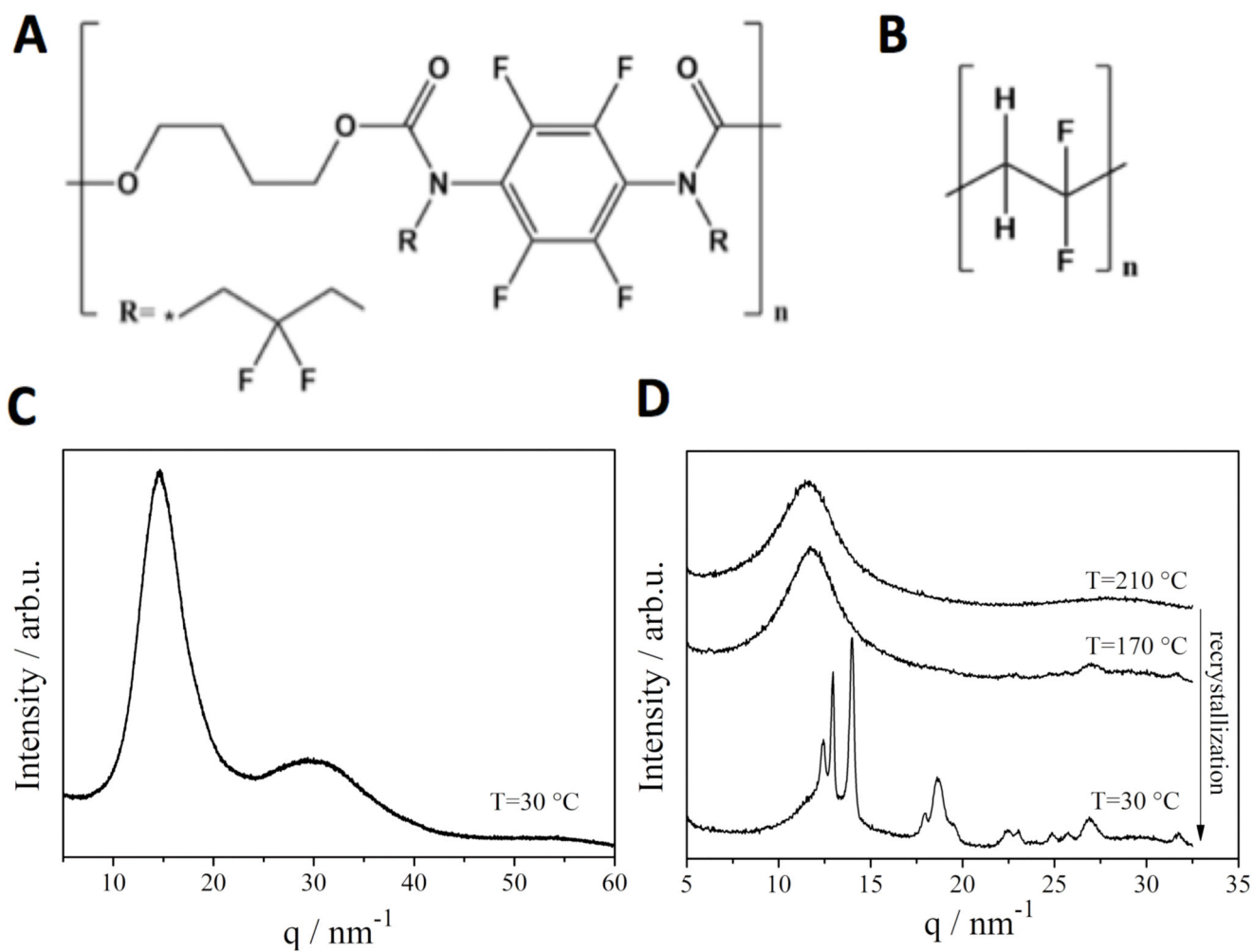


Figure 2. Chemical structure and wide-angle X-ray scattering (WAXS) diffractograms of ^{19}F -TPU (A and C) and PVDF (B and D), exemplifying the amorphous character of ^{19}F -TPU and the high crystallinity of PVDF.

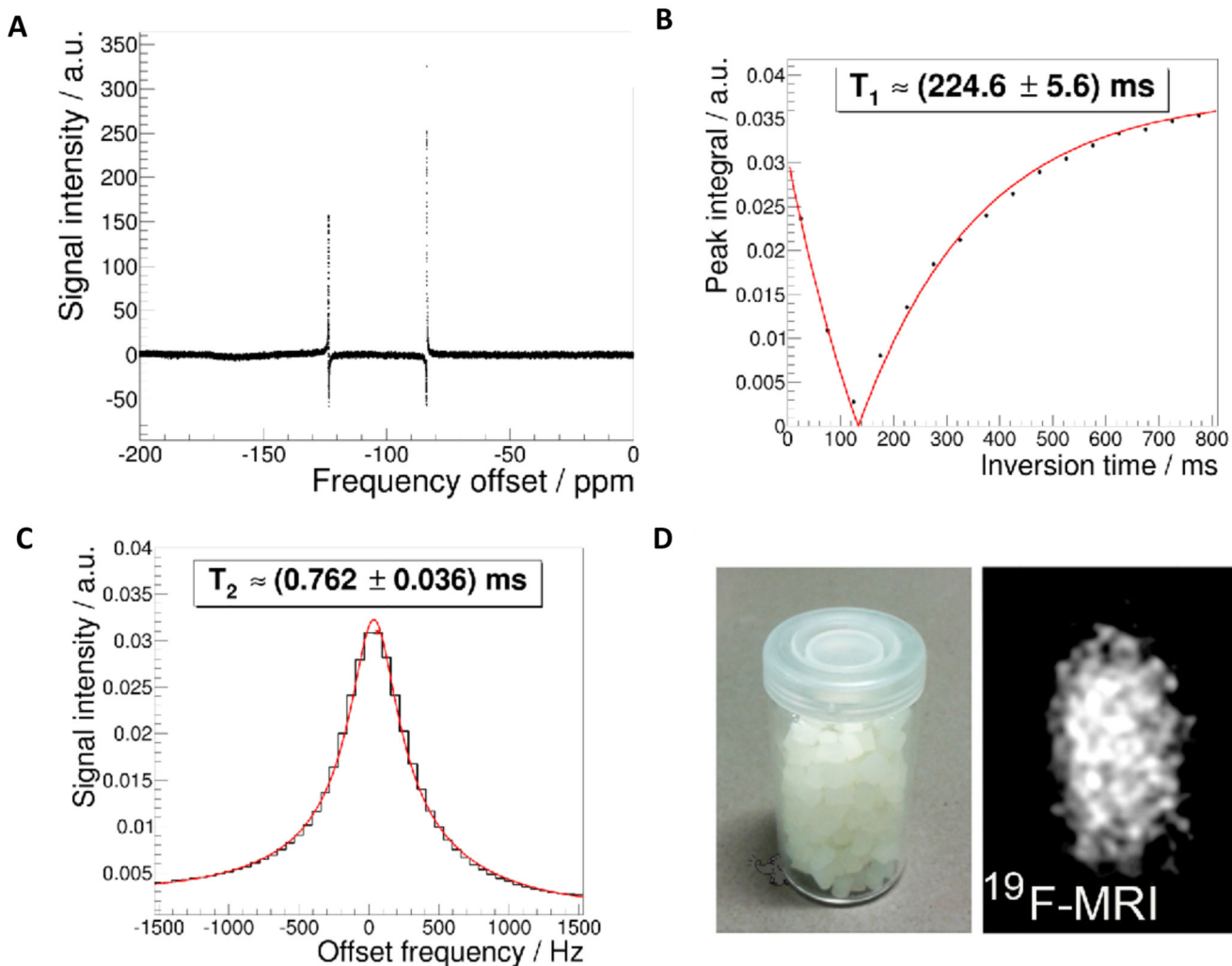


Figure 3.

MRI characterization of ^{19}F -TPU. A: ^{19}F -NMR spectra of the polymeric solution with deuterated chloroform as solvent, recorded using a Bruker DPX-400 FT-NMR spectrometer at 376.5 MHz. B-C: T_1 and T_2 measurements. Please note that only the strongest ^{19}F -peak has been used for imaging due to the large spectral separation (~ 40 ppm) of the two ^{19}F peaks (A) and acquisition bandwidth of 8 kHz of the clinical 3T MRI scanner. D: ^{19}F MR imaging of ^{19}F -TPU polymeric pellets in a 3T scanner using an UTE sequence.

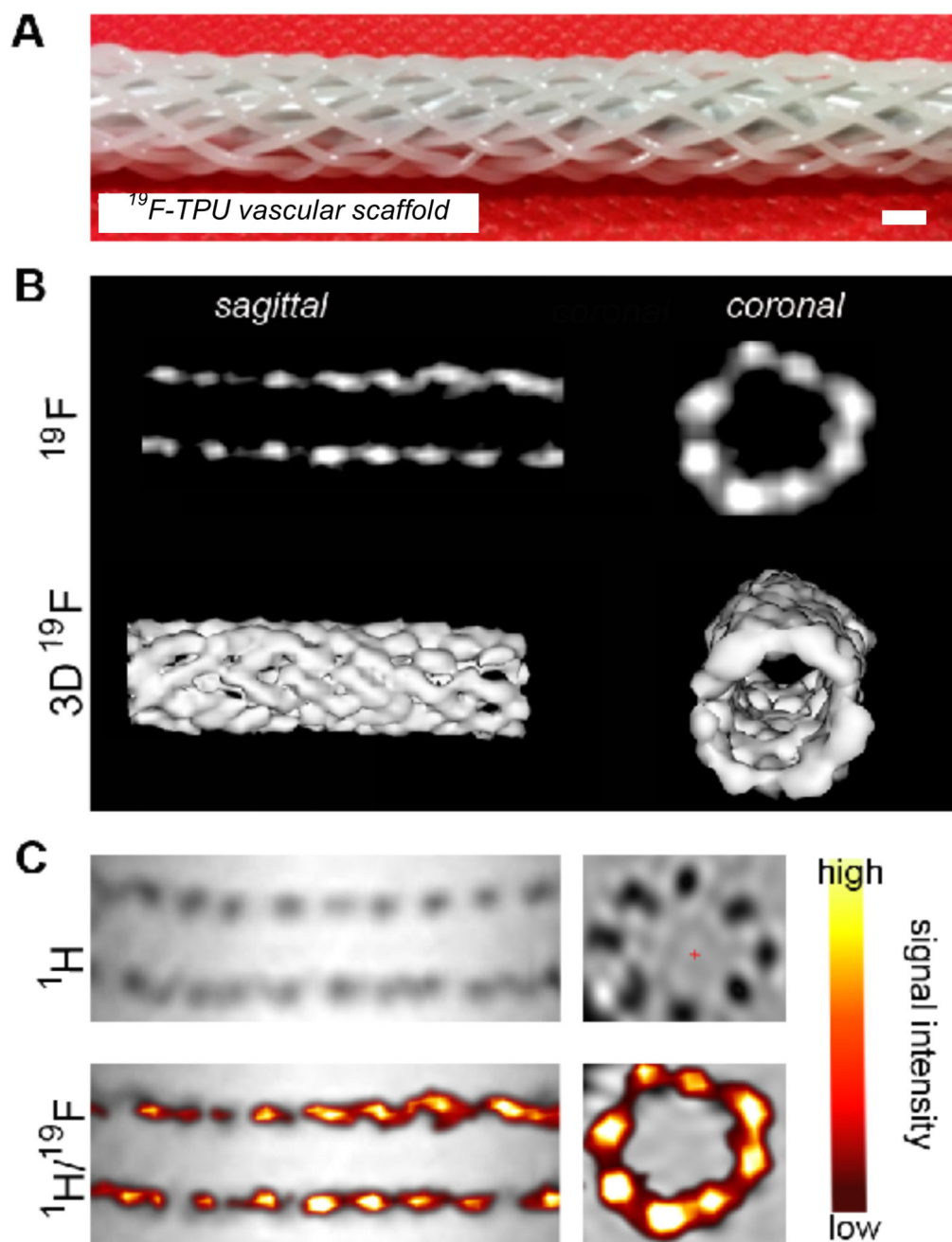


Figure 4. ^{19}F -TPU-based vascular scaffold, enabling ‘hot spot’ MRI and 3D rendering. A: Photographic image of the braided vascular scaffold structure. Scale bar: 2 mm. B: ^{19}F MRI of the scaffold in sagittal and coronal planes (top) and upon 3D rendering (bottom). C: ^1H MRI (top) and $^1\text{H}/^{19}\text{F}$ MRI overlay images (bottom) of the ^{19}F -TPU scaffolds.